

Astrometric Microlensing: A Channel to Detect Multiple Lens Systems

Cheongho Han^{*}

Department of Physics, Institute for Basic Science Research, Chungbuk National University, Cheongju 361-763, Korea

2 November 2018

ABSTRACT

If a source star is gravitationally microlensed by a multiple lens system, the resulting light curve can have significant deviations from the standard form of a single lens event. The chance to produce significant deviations becomes important when the separations between the component lenses are equivalent to the combined angular Einstein ring radius of the system. For multiple lens systems composed of more than two lenses, however, this condition is difficult to meet because the orbits of such systems are unstable. Even if events are caused by a multiple lens system with stable orbits where a pair of lenses are closely located and the other component (third body) has a wide separation from the pair, photometrically identifying the lens multiplicity will be difficult because the event will be identified either by a binary lens event caused by the close pair lenses or a single lens event caused by the third body. In this paper, we show that if a seemingly binary lens event is astrometrically followed up by using future high precision interferometers, the existence of an additional third body can be identified via a repeating event. We show that the signatures of third bodies can be unambiguously identified from the characteristic distortions they make in the centroid shift trajectories. We also show that due to the long range astrometric effect of third bodies, the detection efficiency will be considerable even for third bodies with large separations from their close lens pairs.

Key words: gravitational lensing – binaries: general

1 INTRODUCTION

If a source star is gravitationally microlensed by a multiple lens system, the resulting light curve can have significant deviations from the standard form of a single lens event. The chance to produce significant deviations induced by the lens multiplicity becomes important when the separations between the component lenses are comparable to the combined Einstein ring radius of the system, which is related to the physical parameters of the lens system by

$$\theta_E = \left[\frac{4Gm_{\text{tot}}}{c^2} \left(\frac{1}{D_{\text{ol}}} - \frac{1}{D_{\text{os}}} \right) \right]^{1/2}, \quad (1)$$

where $m_{\text{tot}} = \sum_i^N m_i$ is the total mass of the lens system, N is the total number of the component lenses, m_i are the masses of the individual lenses, and D_{ol} and D_{os} are the distances to the lens system and the source star, respectively. Some fraction of binary lens systems can meet this requirement, and dozens of candidate binary lens events have been reported by the lensing survey and followup observations (Udalski et al. 1994; Dominik & Hirshfeld 1994; Alard, Mao & Guibert 1995; Alcock et al. 2000; Afonso et al. 2000; Albrow et al. 2000).

However, for multiple lens systems that are composed of more than two lenses, it is difficult to photometrically identify the lens multiplicity. There are two reasons for this. First, multiple systems with all constituent lenses having separations between them equivalent to θ_E are very rare because the orbits of such systems are unstable. Second, even if events are caused by a multiple lens system with stable orbits where a pair of lenses are closely located and the other component (third body) has a wide separation from the pair, the close pair and the third body will behave as if they are two independent lens systems, causing the event to be identified either by a binary lens or a single lens event. One case the lens multiplicity can be identified is when the source trajectory approaches closely both the close lens pair and the third body, causing a repeating event. However, due to the short range photometric effect of the third body, the chance to produce repeating events is very low (see § 3). Although there was a claim that a triple lens system was discovered by Bennett et al. (1999), it was subsequently shown to be better explained by a rotating binary (Albrow et al. 2000). As a result, despite the substantial fraction of multiple systems (Evans 1968; Batten 1973; Batten & Fletcher 1989; Fekel 1981; Mayor & Mazeh 1987), not a single multiple lens event has been reported to date.

^{*} e-mails: cheongho@astroph.chungbuk.ac.kr (CH)

Until now, lensing observations have been carried out only photometrically. However, by using several planned high precision optical interferometers, such as those to be mounted on space-based platforms, e.g. the *Space Interferometry Mission* (SIM) and the *Global Astrometric Interferometer for Astrophysics* (GAIA), and those to be mounted on very large ground-based telescopes, e.g. Keck and VLT, it will become possible to observe lensing events astrometrically. When an event is astrometrically observed by using these instruments, one can measure the lensing induced displacement of the source star image centroid position with respect to its unlensed position (centroid shift δ). Astrometric lensing observation is important because the lens mass can be better constrained with the measured centroid shift trajectory (Miyamoto & Yoshii 1995; Walker 1995; Paczyński 1998; Boden, Shao & van Buren 1998).

In this paper, we show that astrometric lensing can also be used for efficiently detecting third bodies in multiple lens systems. This is possible because due to the long range astrometric effect of third bodies, the lens multiplicity of a large fraction of events can be identified via repeating events. We investigate the properties of the deviations induced by third bodies in the centroid shift trajectories of events and estimate the efficiency of third body detections expected from the future lensing observations. We note that this paper is extension of the work of Han et al. (2002) who recently demonstrated the high efficiency of astrometric lensing observations in detecting very wide binary companions.

2 BASICS OF MULTIPLE LENSING

If a source star is lensed by a multiple lens system, the locations of the resulting images are obtained by solving the lens equation. When all lengths are normalized by the combined Einstein ring radius, the lens equation is expressed in complex notations by

$$\zeta = z + \sum_i^N \frac{m_i/m_{\text{tot}}}{\bar{z}_i - \bar{z}}, \quad (2)$$

where z_i are the positions of the lenses, $\zeta = \xi + i\eta$ and $z = x + iy$ are the positions of the source and images, and \bar{z} denotes the complex conjugate of z (Witt 1990). The magnifications of the individual images are given by the inverse of the determinant of the Jacobian of the lens equation evaluated at the image position, i.e.

$$A_j = \left(\frac{1}{|\det J|} \right)_{z=z_j}; \quad \det J = 1 - \frac{\partial \zeta}{\partial \bar{z}} \frac{\partial \bar{\zeta}}{\partial z}. \quad (3)$$

Then the total magnification and the source star image centroid shift are obtained by

$$A = \sum_j^{N_I} A_j, \quad (4)$$

and

$$\delta = \frac{\sum_j^{N_I} A_j \mathbf{z}_j}{A} - \zeta, \quad (5)$$

where $\zeta = (\xi, \eta)$ and $\mathbf{z}_j = (x_j, y_j)$ are the vector notations for the source and image positions and N_I represents the number of images. Since the lens equation describes a mapping from the lens plane onto the source plane, to find the

image positions for given positions of the source and the lenses, it is required to invert the lens equation.

For a single lens system ($N = 1$), the lens equation can be simply inverted. Algebraically solving the lens equation yields two solutions of the image positions, and the total magnification and the centroid shift are expressed in simple forms of

$$A = \frac{u^2 + 2}{u\sqrt{u^2 + 4}}, \quad (6)$$

and

$$\delta = \frac{\mathbf{u}}{u^2 + 2} \theta_E, \quad (7)$$

where \mathbf{u} is the dimensionless lens-source separation vector normalized by θ_E . For a single lens event, the light curve has a smooth symmetric shape (Paczynski 1986) and the centroid shift follows an elliptical trajectory (Walker 1995; Jeong, Han & Park 1997).

For a multiple lens system ($N \geq 2$), on the other hand, the lens equation is non-linear and thus cannot be analytically inverted. However, since the lens equation can be expressed as a polynomial in z , the image positions are obtained by numerically solving the polynomial. For a N point-mass lens system, the lens equation is equivalent to a $(N^2 + 1)$ -order polynomial in z and there are a maximum $N^2 + 1$ and a minimum $N + 1$ images and the number of images changes by a multiple of two as the source crosses a caustic (Rhie 1997; Witt 1990). The caustic is the main new feature of the multiple lens system, which refers to the source position on which the magnification of a point source event becomes infinity. For a binary lens system ($N = 2$), the sets of caustics form close curves. For a multiple lens system, the caustic structure becomes more complex and can exhibit self-intersecting and nested shapes. The order of the polynomial rapidly increases as the number of lenses increases, and thus it becomes difficult to directly solve the equation for systems composed of many lenses. One commonly used numerical method that allows one to study the lensing behaviors of multiple lens systems regardless of the number of lenses is the ‘‘inverse ray-shooting method’’ (Schneider & Weiss 1986; Kayser, Refsdal & Stabell 1986; Wambsganss 1997). The disadvantage of using this method is that it requires large computation time to study the detailed structures in the patterns of magnifications and centroid shifts.

In our analysis, we investigate the lensing properties of triple lens systems instead of testing systems with various numbers of lenses. We note, however, that for systems composed of more than three lenses, the individual sets of lenses composed of the close pair lenses and each of the widely separated companion, in most cases, can be treated as independent triple lens systems. In addition, for triple lens systems, one can directly solve the lens equation instead of using the very time-consuming inverse ray-shooting method.

3 PROPERTIES OF MULTIPLE LENSING BEHAVIORS

If a lens system contains an additional third body, the lensing behavior of the lens system is affected by the third body. The most important effect of the third body is that it makes the effective positions of other lens components shifted towards it. The approximate amount of the shift is

$$\Delta z_i = \frac{q_T}{d} \frac{\mathbf{r}_3}{|\mathbf{r}_3|}, \quad (8)$$

where \mathbf{r}_3 is the position vector of the third body from the center of mass of the two close pair lenses (hereafter binary center), $d = |\mathbf{r}_3|/\theta_{E,B}$ is the separation between the third body and the binary center normalized by the combined Einstein ring of the two close pair lenses, $\theta_{E,B} = [4G(m_1 + m_2)/c^2][(1/D_{ol}) - (1/D_{os})]^{1/2}$, and $q_T = m_3/(m_1 + m_2)$ is the ratio of the third body mass to the total mass of the close pair lenses. If this effect is taken into consideration, however, the photometric lensing behavior of events during the time when the source passes the region around the close lens pair is well approximated by that of the binary lens events without the third body. Similarly, besides the inverse effective positional shift of the third body towards the close lens pair, the lensing behavior of events during the source's approach to the third body is well approximated by that of the single lens event caused solely by the third body. That is, the close lens pair and the third body behave as if they are two independent lens systems. In addition, since the photometric effect of both the close lens pair and the third body are confined to narrow regions around the individual lens systems, even if an event is caused by a triple lens systems, the event, in most cases, will be identified either by a binary lens or a single lens event.

However, if a seemingly binary lens event is astrometrically followed up, the existence of an additional third body can be identified with a significantly increased efficiency. This is because, compared to the photometric effect, the astrometric effect of the third body endures to a large distance from it (Miralda-Escudé 1996), and thus it can cause noticeable deviations in the trajectories of the source star image centroid shifts even when the source approaches the third body with a considerable separations.

To show this, we construct maps of excess magnifications and centroid shifts of an example triple lens system. The excess magnification and the centroid shift are defined respectively by

$$\epsilon = \frac{A_T - A_B}{A_T}, \quad (9)$$

and

$$\Delta\delta = \delta_T - \delta_B, \quad (10)$$

where A_T and δ_T represent the magnification and the centroid shift of the exact triple lens system, while A_B and δ_B represent those of the binary lens event without the third body. The constructed maps are presented in Figure 1. For the construction of the maps, we take the effect of the positional shifts induced by the third body into consideration. The two close pair lenses of the triple lens system have a mass ratio of $q_B = m_2/m_1 = 1.0$ and the separation between them is $a_B = 1.0$ in units of $\theta_{E,B}$. The third body has a mass ratio of $q_T = 0.6$ and it is separated from the binary center by $a_T = 15.0$ (also in units of $\theta_{E,B}$ [†]) with an orientation angle of 45° with respect to the axis connecting the two close pair lenses. The locations of the lenses are marked by filled dots on the maps. Grey scales are used to represent the regions of deviations with $\epsilon \geq 5\%$, 10% , and 20% for the excess magnification map and $\Delta\delta \geq 5\%$, 10% , and 20% of $\theta_{E,B}$ for the excess centroid shift map. The coordinates of the maps are centered at the center of the mass of the close pair lenses and all lengths are normalized by $\theta_{E,B}$. The straight lines with arrows represent the source trajectories of events whose light curves and centroid shifts are presented in Fig. 2. The solid curve near the close lens pair represents the caustics. The inset in each panel shows the enlarged view of the map in the region around the close pair lenses. The dashed circle in each inset represents the combined Einstein ring of the close pair lenses.

[†] According to the strategy of monitoring binary lens events for third body detections, the event caused by the close pair lenses will be the standard of all measurements. Therefore, we normalize all lengths and time scales in units of $\theta_{E,B}$ and $t_{E,B}$, where $t_{E,B}$ is the time required for the source to transit $\theta_{E,B}$.

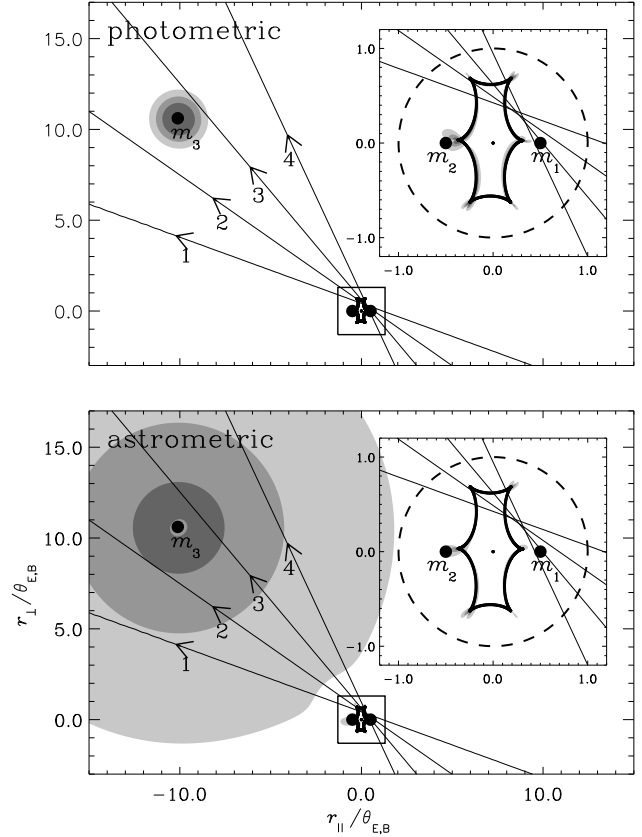


Figure 1. The maps of excess magnification (upper panel) and centroid shift (lower panel) of an example multiple lens system. The lens system is composed of three lenses where a pair of lenses are closely located and the other component (third body) is widely separated from the pair. The two close pair lenses have a mass ratio of $q_B = m_2/m_1 = 1.0$ and they are separated by $a_B = 1.0$ in units of $\theta_{E,B}$. The third body has a mass ratio of $q_T = m_3/(m_1 + m_2) = 0.6$ and separated from the center of mass of the close pair lenses by $a_T = 15.0$ also in units of $\theta_{E,B}$. The filled dots represent the locations of the three lenses. Grey scales are used to represent the regions of deviations with $\epsilon \geq 5\%$, 10% , and 20% for the excess magnification map and $\Delta\delta \geq 5\%$, 10% , and 20% of $\theta_{E,B}$ for the excess centroid shift map. The coordinates of the maps are centered at the center of the mass of the close pair lenses and all lengths are normalized by $\theta_{E,B}$. The straight lines with arrows represent the source trajectories of events whose light curves and centroid shifts are presented in Fig. 2. The solid curve near the close lens pair represents the caustics. The inset in each panel shows the enlarged view of the map in the region around the close pair lenses. The dashed circle in each inset represents the combined Einstein ring of the close pair lenses.

$\theta_{E,B}$ for the excess centroid shift map. For a typical Galactic lensing event, the angular Einstein ring radius is $\sim (\mathcal{O})10^2 \mu\text{-arcsec}$, and thus $\Delta\delta = 0.1\theta_{E,B}$ corresponds to $\sim (\mathcal{O})10 \mu\text{-arcsec}$. For comparison, we note the SIM will be able to measure positional shifts of stars as small as several $\mu\text{-arcsec}$ (<http://sim.jpl.nasa.gov>).

From Fig. 1, one finds the following facts. First, due to the large separation between the third body and the close lens pair, both the photometric and astrometric effects of the third body are not important in the region around the close lens pair, implying that not only the photometric but also the astrometric lensing behaviors of triple lens events

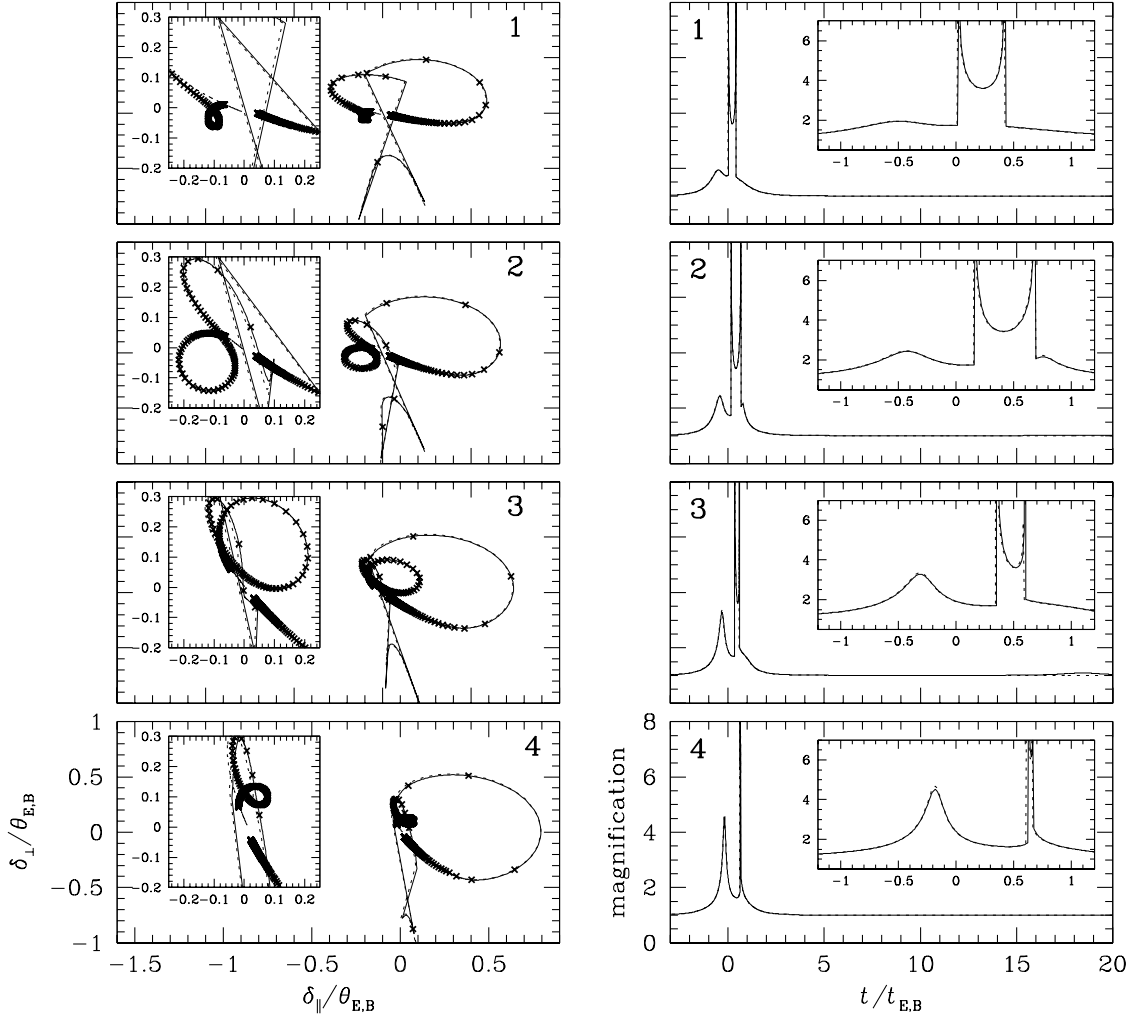


Figure 2. Example centroid shift trajectories (left panels) and light curves (right panels) of events caused by the triple lens system whose maps of excess magnification and centroid shift are presented in Fig. 1. The source trajectories responsible for the individual events are marked in Fig. 1, where the number in each panel corresponds to that of the source trajectory. In each panel, the dotted and solid curves represent the centroid shift trajectories and light curves produced with and without the third body. The insets inside the left side panels show the detailed structures of the centroid shift distortions induced by the third body. The insets inside the right side panels show the enlargement of the part of the light curve during the source’s passages around the region of the close lens pair.

during the source’s passage of the region around the close lens pair are well described by the binary lensing approximation. Second, the region of significant astrometric deviations around the third body is much larger than the region of significant photometric deviations, implying that for an important fraction of multiple lens events the existence of third bodies can be identified from extended astrometric followup lensing observations.

To see the characteristics of the photometric and astrometric deviations induced by the third body, in Figure 2, we present the light curves and the centroid shift trajectories of several events caused by the triple lens system. The source trajectories responsible for the individual events are marked in Fig. 1. In each panel, we also present the curves of the binary lens events computed without the third body taking the effective positional shifts of the close binary lens pair into consideration (dotted curves). On the centroid shift trajectories, we mark the centroid positions (‘x’ symbols) measured with a time interval of $t_{E,B}/4$ to show the changing rate of

the centroid position. For an event with $t_{E,B} \sim 1$ month, therefore, this interval corresponds to roughly a week. From the comparison of the centroid shift trajectories and the light curves of the corresponding events, one finds that the astrometric signatures of the third body can be clearly identified from the characteristic loop-shaped distortions in the centroid shift trajectories, while the photometric signatures are too weak to be noticed. One also finds that the astrometric deviations last for a long period of time.

4 EFFICIENCY OF THIRD DETECTIONS

In the previous section, we showed that astrometric lensing observations will enable one to identify the third body of a multiple lens system with little ambiguity from the characteristic deviations it makes in the centroid shift trajectories. In this section, we determine the efficiency of detecting third bodies expected from the future astrometric lensing observations. For this determination, we use the formalism intro-

duced by Di Stefano & Scalzo (1999) and further developed by Han et al. (2002).

If we define b_B and b_3 as the smallest separations from the source trajectory to the binary center and the third body, the orientation angle of the source trajectory with respect to the line connecting the binary center and the third body is represented by

$$\alpha_{\pm} = \sin^{-1} \left(\frac{b_B \pm b_3}{|r_3|} \right), \quad (11)$$

where the sign ‘-’ is for the case when the closest points on the source trajectory from the binary center and the third body are on the same side with respect to the line connecting the binary center and the third body, and the ‘+’ sign is when the closest points are on the opposite sides. If all lengths are normalized in units of $\theta_{E,B}$, equation (11) is expressed by

$$\alpha_{\pm} = \sin^{-1} \left(\frac{\beta_B \pm \sqrt{q_T} \beta_3}{d} \right), \quad (12)$$

where β_B and β_3 are the lensing impact parameters of the two independent events involved with the binary system composed of the close pair lenses and the single third body, respectively.[‡] Let us additionally define $\beta_{3,th}$ such that among events that were identified to be affected by the close lens pair by approaching the binary center with an impact parameter β_B , only events with source trajectories passing the third body closer than $\beta_{3,th}$ can be identified as multiple lens events from the centroid shift deviations larger than a threshold value $\Delta\delta_{th}$. Then, the fraction of multiple lens events whose third bodies can be astrometrically identified is computed by

$$P = \frac{\alpha_{+,th} - \alpha_{-,th}}{\pi}, \quad (13)$$

where the threshold orientation angles have values

$$\begin{cases} \alpha_{+,th} = \sin^{-1} \left(\frac{\beta_B + \sqrt{q_T} \beta_{3,th}}{d} \right) \\ \alpha_{-,th} = \sin^{-1} \left(\frac{\beta_B - \sqrt{q_T} \beta_{3,th}}{d} \right) \end{cases} \quad (14)$$

for $d > \beta_B + \sqrt{q_T} \beta_{3,th}$,

$$\begin{cases} \alpha_{+,th} = \pi/2 \\ \alpha_{-,th} = \sin^{-1} \left(\frac{\beta_B - \sqrt{q_T} \beta_{3,th}}{d} \right) \end{cases} \quad (15)$$

for $|\beta_B - \sqrt{q_T} \beta_{3,th}| < d \leq \beta_B + \sqrt{q_T} \beta_{3,th}$, and

$$\begin{cases} \alpha_{+,th} = \pi/2 \\ \alpha_{-,th} = -\pi/2, \end{cases} \quad (16)$$

for $d \leq |\beta_B - \sqrt{q_T} \beta_{3,th}|$. We note that the threshold orientation angles have different values depending on the relative size of the astrometrically effective region of the third body compared to the separation between the third body and the binary center. For a given value of the threshold centroid shift deviation, $\Delta\delta_{th}$, the corresponding threshold impact parameter to the third body is obtained by

[‡] By definition, the lensing impact parameter represents the closest separation between the source trajectory to the lens (the center of mass of the lens system) normalized by the (combined) angular Einstein ring radius of the involved lens (lens system), and thus $\beta_B = b_B/\theta_{E,B}$ and $\beta_3 = b_3/\theta_{E,3}$, where $\theta_{E,3}$ represents the Einstein ring radius of the third body.

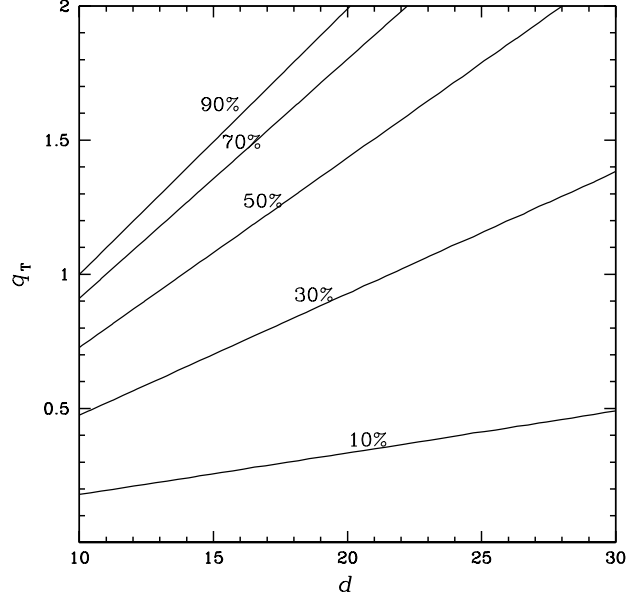


Figure 3. The expected efficiency of detecting third bodies from astrometric followup lensing observations as functions of the separation, d , and the mass ratio, q_T , between the third body and the close lens pair. We assume that a third body is detected if the deviation induced by the third body is larger than 10% of the combined angular Einstein ring radius of the monitored binary lens event, $\theta_{E,B}$. The separation is expressed in units of $\theta_{E,B}$.

$$\beta_{3,th} = \frac{1}{2} \left(\frac{1}{\Delta\delta_{th}/\theta_{E,3}} + \sqrt{\left(\frac{1}{(\Delta\delta_{th}/\theta_{E,3})^2} - 8 \right)} \right). \quad (17)$$

If one expresses the threshold astrometric deviation in terms of the fraction of the combined Einstein ring radius of the close pair lenses, $f = \Delta\delta_{th}/\theta_{E,B}$, equation (17) becomes

$$\beta_{3,th} = \frac{1}{2} \left(\frac{\sqrt{q_T}}{f} + \sqrt{\frac{q_T}{f^2} - 8} \right). \quad (18)$$

In Figure 3, we present the determined efficiency in the parameter space of the separation and the mass ratio between the third body and the close lens pair, $P(d, q_T)$. For this computation, we set $f = 0.1$. For the impact parameter to the close lens pair, we adopt $\beta_B = 0.0$, but we note that the dependency of the efficiency on the adopted value of β_B is not important as long as $\beta_B \ll d$. We also note that q_T can be larger than 1.0 because the third body can be heavier than the total mass of the close pair lenses. From the figure, one finds that the efficiency is substantial even for third bodies that are widely separated from their close lens pairs. It is worth to note that the scaling between d and q_T are quite linear. This can be understood as follows. The probability of detecting third bodies is proportional to the threshold orientation angle, i.e. $P \propto \alpha \propto \sin^{-1}(\sqrt{q_T} \beta_{3,th}/d)$ [see eq. (12) and (13)]. In the limit of $d \gg \sqrt{q_T} \beta_{3,th}$, $\sin^{-1}(\sqrt{q_T} \beta_{3,th}/d) \sim \sqrt{q_T} \beta_{3,th}/d$, and thus $P \propto \sqrt{q_T} \beta_{3,th}/d$. Since $\beta_{3,th} \propto \sqrt{q_T}$ [see eq. (18)], one finds that $P \propto q_T/d$. Therefore, the scaling between d and q_T is linear.

5 CONCLUSION

In this paper, we show that future astrometric lensing observations will provide an efficient method of detecting third bodies of multiple lens systems, which could not have been detected from conventional photometric lensing observations. We showed that the deviation in the centroid shift trajectory induced by the third body of a multiple lens system has a characteristic loop that can be clearly distinguished from other types of deviations and thus can be unambiguously identified. In addition, since the deviations last for a long period of time, detecting third bodies will be possible even from sparse astrometric sampling.

This work was supported by a grant (BSRI-01-2) from the Basic Science Research Institute of Chungbuk National University.

REFERENCES

- Afonso C., et al., 2000, *ApJ*, 532, 340
Alard C., Mao, S., Guibert J., 1995, *A&A*, 300, L17
Albrow M. D., et al., 2000, *ApJ*, 534, 894
Alcock C., et al., 2000, *ApJ*, 541, 270
Batten A. H., 1973, *Binary and Multiple Systems of Stars* (New York: Pergamon)
Batten A. H., Fletcher J. M., 1989, *J. Roy. Astron. Soc., Can.*, 83, 289
Bennett D. P., et al., 1999, *Nature*, 402, 57
Boden A. F., Shao M., van Buren D., 1998, *ApJ*, 502, 538
Di Stefano R., Scalzo R. A., 1999, *ApJ*, 512, 579
Dominik M., Hirshfeld A. C., 1994, *A&A*, 289, L31
Evans D. S., 1968, *Quarterly J. Roy. Astron. Soc.*, 9., 388
Fekel F. C., 1981, *ApJ*, 246, 879
Han C., Park B.-G., Han W., Kang Y. W., 2002, *ApJ*, 569, 000
Jeong Y., Han C., Park S.-H., 1997, *ApJ*, 511, 569
Kayser R., Refsdal S., Stabell R., 1986, *A&A*, 166, 36
Miralda-Escudé J., 1996, *ApJ*, L113
Miyamoto M., Yoshii Y. 1995, *AJ*, 110, 1427
Mayor M., Mazeh T., 1987, *A&A*, 171, 157
Paczynski B., 1986, *ApJ*, 304, 1
Paczynski B. 1998, *ApJ*, 404, L23
Rhie S. H., 1997, *ApJ*, 484, 63
Schneider P., Weiss A., 1986, *A&A*, 164, 237
Udalski A., Szymański M., Mao, S., di Stefano R., Kaluźny J., Kubiak M., Mateo M., Krzemiński W., 1994, *ApJ*, 436, L103
Walker M. A., 1995, *ApJ*, 453, 37
Wambsgans J., 1997, *MNRAS*, 284, 172
Witt H. J., 1990, *A&A*, 236, 311